Two Methods of Fault Detection in the PMSM Electric Drive IGBT-Based Inverter

NIKITA SMIRNOV, SERGEY TUSHEV
Department of Electrical Engineering and Precision Electromechanical Systems
University ITMO
Kronverkskiy ave., 49, Saint-Petersburg
RUSSIA
N.Smirnov@ets.ifmo.ru, sergy5@mail.ru

Abstract: - The paper considers abnormal operation modes of an electric drive power subsystem with permanent magnet synchronous motor (PMSM), such as breakdown and burnout of IGBT-transistor in the three-phase inverter. The effect of these faults on the spectrum and form of the currents in the windings of the synchronous motor was studied. Heuristic algorithms based on the form features of the winding currents in abnormal conditions were proposed for faults detection.

Key-Words: - Fault Diagnosis; FFT Analysis; PMSM; Electric Drive; Inverter Faults.

1 Introduction

In modern quantum optical systems digital direct servo drive based on a PMSM controlled by a transistor inverter is widely used. Such drive has higher performance compared to a DC drive, including the reliability of its assemblies [1]. As in any technological devices, however, various faults may occur in drive's components during its service, including the power subsystem.

Current waveform distortions in the motor windings resulting from such faults directly affect the control quality of the electric drive and life of the motor, bearings, and semiconductor power inverter. In addition, nonsymmetrical winding currents account for a non-uniform electromagnetic torque, which increases a telescope tracking error up to values exceeding the requirements specification. On account of this, electric drive control system requires fault diagnosis algorithms for preventing the emergency mode operation of the drive.

The electric drive state can be diagnosed either using additional sensors by measuring physical parameters of semiconductor switches and the motor, or estimating their state indirectly according to the information on the currents and voltages in the motor windings already available in the system. Additional sensors complicate the electrical circuit of the power amplifier and increase the time and cost of the electric drive design. Though the significant part of the bibliography highlights mostly the diagnostics of the drives with induction motors [2-9], certain articles are devoted to fault detection in drives based on permanent magnet motors [11]. In this papers study various techniques such as Park's vector approach [3], artificial neural networks [5], Hilbert and Wavelet Transforms [7], Fast Fourier transform (FFT) [8-10], fuzzy logic [11]

An over current protection is most simple to implement in a microprocessor control system. But under various emergency conditions the currents in the motor windings do not exceed the cut-off threshold; therefore it is necessary to make a deeper analysis of the waveform and interrelations of the winding currents. Let us formulate the research task as a development of algorithms for determining the state of semiconductor switches in the inverter, which may be used for preliminary preparation of the drive for operation. As a test signal is used three pulse-width modulated (PWM) voltages supplied to the motor windings through a three-phase voltage fed inverter.

Let's say that electric drive works in open-switch fault mode if one of transistors in the inverter was burnout. If transistor was broken-down we'll say that drive works in short-switch fault mode. At failure of the top or bottom transistor in the inverter symptoms of emergency modes will also differ.

2 Mathematical Model

To investigate winding currents form during various faults in the operation of the power switch in the inverter, and to synthesize algorithms, let's take system of differential equations describing model of single-mass model of electric drive with PMSM.

ISBN: 978-960-474-371-1

Equations of interrelation of winding currents and voltage in PMSM and electromagnetic torque and speed of drive are presented below (1).

$$\begin{cases} Ri_a + L\dfrac{d}{dt}(2i_a - i_b - i_c) - C_e\omega Cos(p_p\varphi) = u_a \\ Ri_b + L\dfrac{d}{dt}(2i_b - i_a - i_c) - C_e\omega Cos(p_p\varphi + \dfrac{2\pi}{3}) = u_b \\ Ri_c + L\dfrac{d}{dt}(2i_c - i_a - i_b) - C_e\omega Cos(p_p\varphi - \dfrac{2\pi}{3}) = u_c \\ T = C_e(i_a cos(p_p\varphi) + i_b cos(p_p\varphi + \dfrac{2\pi}{3}) + \\ + i_c cos(p_p\varphi - \dfrac{2\pi}{3})) \\ \dfrac{d\varphi}{dt} = \omega \\ J\dfrac{d\omega}{dt} = T - T_c \end{cases} \quad (1)$$

Where u_a, u_b, u_c, i_a, i_b, i_c are motor phase voltages and currents; R and L are resistance and inductance of one phase in motor; ω and φ are rotary speed and angle of the rotor; C_e is back EMF constant; p_p is the number of the PMSM stator pole pairs.; T and T_c are electromagnetic and resistance torques and J is rotor inertia. Block diagram of test model in Matlab Simulink package is presented in Fig. 1. *3_sin* block forms three sine curves on the basis of the information on the required phase and amplitude of the sine curves by algorithm presented in (2).

$$\begin{cases} s_a = \gamma \sin\left(p_p\varphi\right) \\ s_b = \gamma \sin\left(p_p\varphi + 2\pi/3\right) \\ s_c = \gamma \sin\left(p_p\varphi - 2\pi/3\right) \end{cases} \quad (2)$$

Where γ is coefficient corresponding to the desired PWM duty cycle; s_a, s_b, s_c are sinusoidal signals formed for *PWM* block. The value of γ applied to the *Gamma* input of the *3_sin*. When simulating drive operation as a part of closed control system, the duty cycle is calculated on the basis of feedback values and required angle and angular velocity. Using a switch, the model is closed by the rotor angle and operates in BLDC mode, or is opened and operates in rotating magnetic field mode.

The *PWM* block forms PWM pulses by a nonsymmetrical law with carrier frequency of 4 kHz. The pulses are supplied to the input of the IGBT-inverter. The three-phase bridge IGBT-inverter was modeled by *Universal Bridge* block from SimPowerSystems library of Matlab Simulink.

Structure of the IGBT-inverter and scheme of its connection to windings of the PMSM are presented on Fig 3. Parameters of IGBT transistor are presented in Table 1. From the inverter the modulated voltage is supplied to the input of the *Drive* block presented in Fig 2. In this block the three-phase PMSM (modeled in the *Motor* block) connecting with a single-mass mechanism by equations (1). A switch disruption or burnout in the inverter was simulated by a setting 1 or 0 respectively, in the control channel of this IGBT-transistor. The simulated currents in the motor windings were stored into the Matlab operating area and the hard drive.

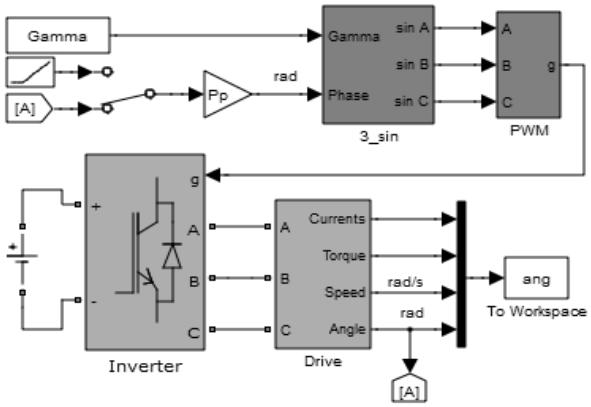

Fig.1 Block diagram of PMSM drive model

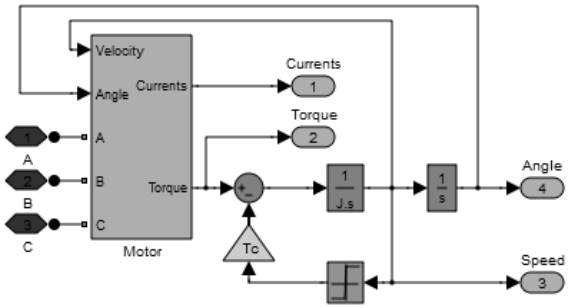

Fig.2 Single-mass model of the electric drive with a PMSM in *Drive* block

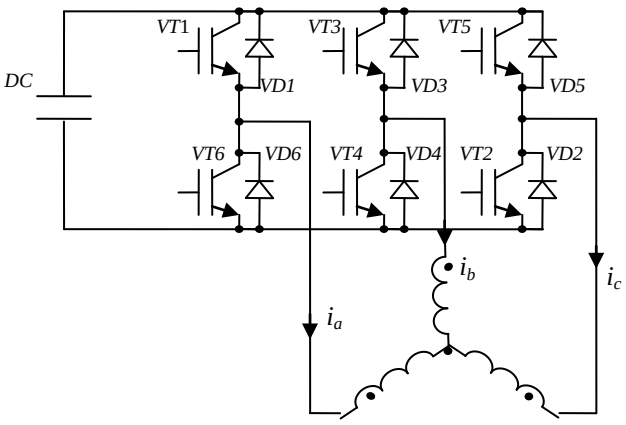

Fig.3 IGBT-inverter.

Table 1. Parameters of IGBT-transistors

Parameter		Value	Units
Snubber resistance	–	1e5	Ohms
Snubber capacitance	–	1e-5	F
Internal resistance	–	1e-3	Ohms
Forward voltage of transistor	–	1.4	V
Forward voltage of diode	–	0.7	V
Current 10% fall time	–	0.4e-6	s
Current tail time	–	0.4e-6	s

3 Fault Detection Using FFT

The simulation was performed in rotating magnetic field mode with the stopped rotor, to exclude the influence of a back EMF. Sample time for modeling in the Matlab Simulink is chosen so as to have 200 points for one period of the inverter carrier frequency, but to Workspace for analysis we write two points for one period of the inverter carrier frequency only. For FFT analysis we take one period of winding currents.

The IGBT-inverter provides the higher harmonics in the spectrum of winding currents. These harmonics introduce significant distortions in the current waveforms even when system's components are healthy. Fig. 4 presents the graphs of winding currents formed by ideal switches (gray) and IGBT (black).

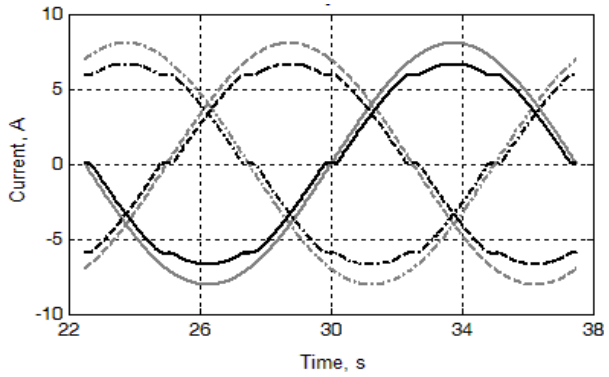

Fig.4 Phase currents at normal operation conditions of power switches with stopped rotor: black – IGBT-inverter; gray – inverter with ideal switches

Let us compare the waveform and spectrum of the currents for the inverter with ideal switches and with IGBT. In the system with inverter with ideal switches the higher harmonics in the FFT expansion of winding currents are negligibly small, and the total harmonic distortion (THD) is 0.07 %, unlike IGBT-inverter (Fig. 5).

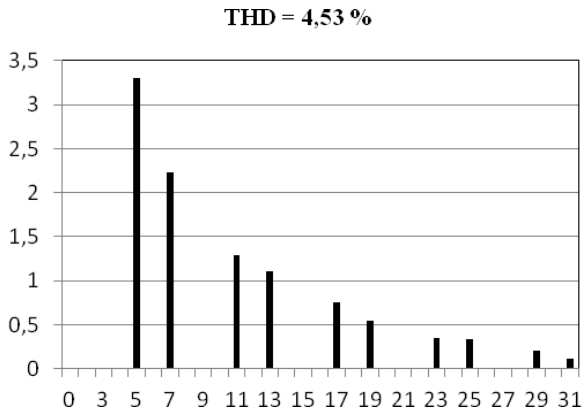

Fig.5 Harmonic amplitudes as a % of fundamental for healthy operation mode of IGBT-inverter

The numbers of the harmonics presented in the currents spectrum of IGBT-inverter can be described by the equation (3).

$$k = 6 \cdot \left| \frac{i}{2} \right| + (-1)^i, i \in \mathrm{N} \qquad (3)$$

Where k is the spectral harmonic number, i is natural number from one to infinity.

Thus, when spectrum of the winding currents are analyzing during various faults, the harmonics characterizing the inverter itself should be taken into account.

The simulation of healthy and emergency operation modes of a power subsystem with different values of the duty cycle and reference frequency of the rotating magnetic field has shown that the spectrum of winding currents is virtually unchanged when the frequency reference varies. At the same time ratio of the first and higher harmonic amplitudes in the spectrum is essentially depends on the duty cycle value. The independence of the spectrum from the reference frequency can be used to reduce the time of preliminary system diagnostics when the drive is preparing for operation by supplying a test signal with a relatively high frequency. To obtain the qualitative result of the FFT expansion, at least one full period of the fundamental harmonic is required (Fig. 6, 7); therefore, the higher reference frequency is, the less time is required for the diagnostics.

Let us discuss how phase currents vary when various faults in the inverter operation are simulating. FFT expansions for winding currents at faulty top (VT1, VT3, VT5 on the Fig. 3) or bottom (VT2, VT4, VT6 on the Fig. 3) transistors in the inverter are similar, so only top transistor fault in inverter arm is presented on next figures.

ISBN: 978-960-474-371-1

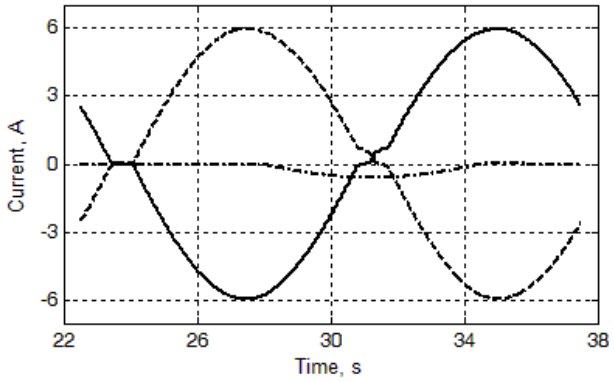

Fig.6 Phase currents at open-switch fault mode with stopped rotor

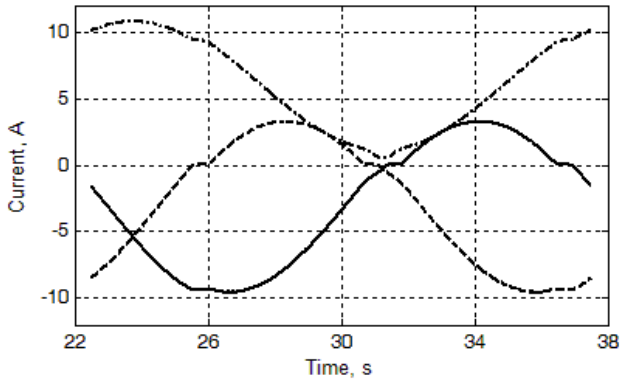

Fig.7 Phase currents at short-switch fault mode with stopped rotor

3.1 Open-switch fault mode

Amplitude values of the harmonics of the winding currents at the burnout transistor are presented in Fig. 8 as percent of fundamental, and THD is the total harmonic distortion.

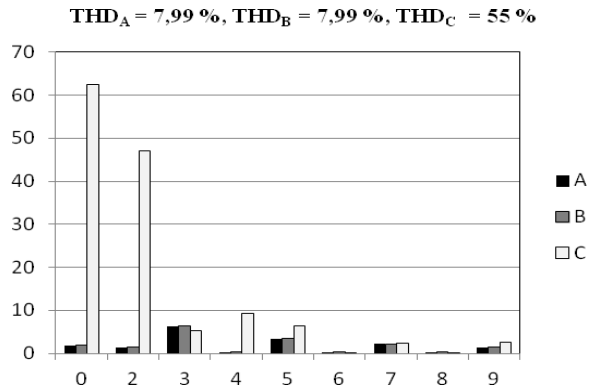

Fig.8 Harmonic amplitudes as a % of fundamental for open-switch fault mode

When the transistor in arm of the inverter is blown (Fig. 6, 8), for part of the period the current does not pass through the phase winding connected to this arm, and the current amplitude is lower than in the remaining phases. The faulty phase has no half-wave of the respective polarity therefore the average current for the period differs from zero. Let us single out the main signs of the open-switch fault mode:

- in the faulty phase the constant component appears equal to about 60 % of the amplitude of the first harmonic on the entire pulse ratio range;
- the current amplitude in the faulty phase is several times less than in the remaining ones;
- the currents spectrum in the healthy phases has a third harmonic;
- the currents spectrum of the faulty phase has 2nd and 4th harmonics;
- THD in the faulty phase exceeds 50%, in the healthy phases it is 80% higher than the normal one;
- when the top transistor was blown, in the faulty phase the angle of the constant component is 180 degrees, in the remaining ones it is 0 degrees, in other words, in the faulty phase the constant component is negative, in the remaining ones it is positive. When the bottom transistor was blown the situation is reversed.

3.2 Short-switch fault mode

Amplitude values of the harmonics of the winding currents at the broken-down transistor are presented in Fig. 9 as percent of fundamental, and THD is the total harmonic distortion.

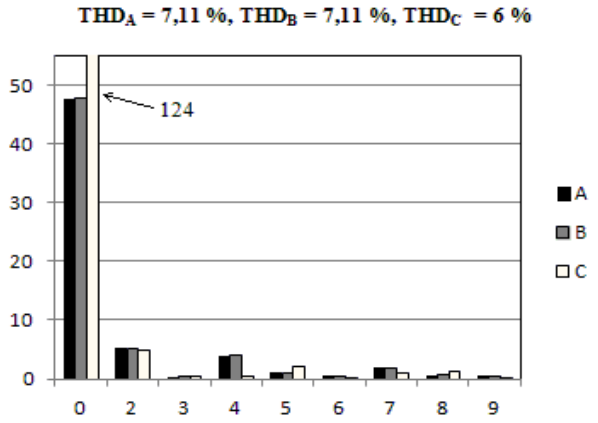

Fig.9 Harmonic amplitudes as a % of fundamental for short-switch fault mode

When there was a breakdown in the transistor (Fig. 7, 9), the arm is constantly connected to the DC voltage of appropriate polarity. Such mode is dangerous because part of the period in the inverter circuit shorts the primary power source (PS). If the current is limited in the connection circuit of the transistor module to the PS, the overcurrent protection of the PS may not be triggered, and the source will operate with an increased load. In terms of the currents in the motor windings such mode is characterized by the following signs:

ISBN: 978-960-474-371-1

- the constant components are significant, the constant component in the faulty phase is almost 3 times higher than in the remaining ones for the entire pulse ratio range;

- at the top broken-down transistor in the faulty phase the angle of the constant component is 0 degrees, in the remaining ones it is 180 degrees (in the faulty phase the constant component is positive, in the remaining ones it is negative). In the bottom broken-down transistor the situation is reversed;

- the currents spectrum has a second harmonic – from 0.75% when the duty cycle is 1 to 5.79% when the duty cycle is 0.2 for the faulty phase and from 0.81% when the duty cycle is 1 to 6.03% when the duty cycle is 0.2 for the remaining phases.

The aggregate of the above signs unambiguously denotes this or that fault of the power subsystem. As the test diagnostic measures are performed when the drive is being prepared for operation, not in the operating mode, there is no necessity of real time data processing. Therefore, the computationally costly harmonic analysis can be affected on an up-stream computer under the control of a general purpose operating system.

4 Fault Detection in the Inverter without using FFT

When the motor shaft is not stopped, a back EMF starts to operate in the windings, directed opposite to the applied voltage and depending on the velocity of the motor shaft. Under the influence of back EMF when the motor shaft run up to constant velocity the winding currents amplitude is reduced to the value corresponding to the torque on the shaft (Fig. 10, 11, 12).

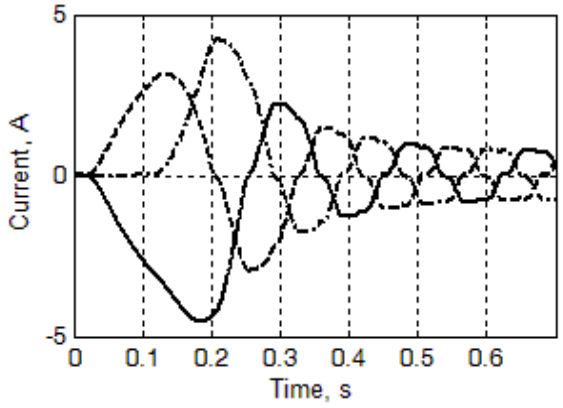

Fig.10 Phase currents for normal operation mode with rotating rotor; unbroken line is phase A, dashed line is phase B, dash-and-dot line is phase C

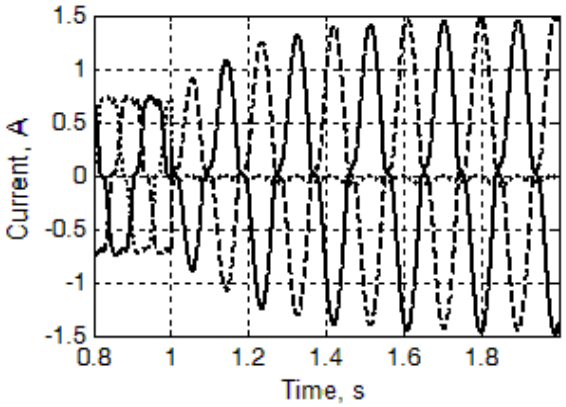

Fig.11 Phase currents for open-switch fault operation mode with rotating rotor; unbroken line is phase A, dash line is phase B, dash-and-dot line is phase C

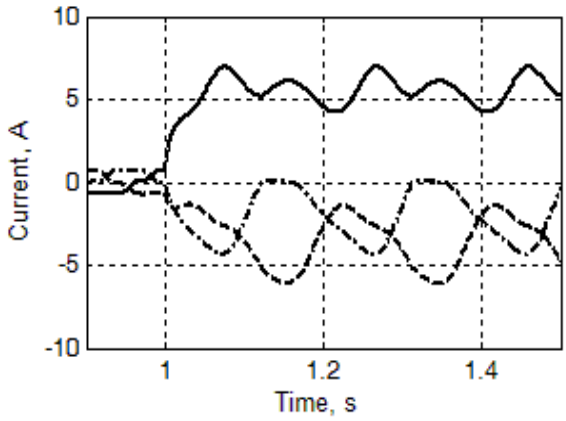

Fig.12 Phase currents for short-switch fault operation mode with rotating rotor; unbroken line is phase A, dash line is phase B, dash-and-dot line is phase C

Let us look at the graphs of currents in phases presented in Fig. 11, 12. For a rotating rotor the duty cycle equals 0.5 was applied, which corresponds to the half of the maximum voltage. The velocity of the drive in the steady-state mode is 88 angular degrees per second. After the motor acceleration to the steady-state value at the moment of time 1 second the emergency in the IGBT-transistor of the inverter arm was simulated.

4.2 Short-switch fault mode.

When the top transistor is shorted in the inverter arm (Fig. 7, 12), the average current in the faulty phase has non-zero value and shifts to the positive area, and the average currents in other phases become negative and their sum is equal in absolute value to the average current in the faulty phase. The shorting of the bottom transistor in the inverter frame provides a mirror image. The average values do not depend on the reference and are determined

ISBN: 978-960-474-371-1

by the resistance of the electric circuit and the parameters of the power source. For this model the average current in the faulty phase is 5.72 A, in the two other phases the average currents are equal to each other, –2.86 A. Thus, the breakdown of transistor in the inverter characterized by the presence in the phase currents of non-zero average components above the certain value.

With the movement of the rotor (Fig. 12) the currents start to have constant components. In the faulty phase the constant component equals 5.51 A. In two other phases constant components equal –1.71 A and –3.8 A. As is seen, in the faulty phase the constant component has grown insignificantly, and in the two other ones the direct currents have been redistributed.

4.3 Open-switch fault mode.

In the open-switch fault mode, for part of the switching period the current does not pass through the inverter arm, therefore there is no corresponding arm of the current curve (Fig. 8, 11). As the second switch in the arm is in operating condition, for the remaining part of the period the arm is open, and the current flows through it in the corresponding direction. The average current in the faulty phase differs from zero and is shifted downward if the high switch is open or upwards if the low switch is open. In the two other phases the currents are virtually symmetrical, differing only by the current value in the faulty phase. The faulty phase is characterized by the presence of only the positive or negative current half-wave and the amplitude which is several times lower than in the two other motor phases. The area under the graph of the faulty phase current is within 1 to 10 percent of the area under the graph of the healthy phase graph.

In the moving drive (Fig. 11) the current amplitude in the healthy windings increases, a negative pulsating current appearing in the faulty phase. The ratios between the current amplitudes in the faulty and healthy phases have remained the same.

4.3 Implementation of the algorithm.

The said differences in the current waveforms can be formalized for each case.

As an example, let us put down these algorithms for the bottom transistor of the third arm. Short-switch fault mode is presented in (4) and open-switch fault mode is presented in (5). Where I_{av}^{A}, I_{av}^{B}, I_{av}^{C} are the average phase currents for the period, S_{+}^{N} and S_{-}^{N} are the areas under the graph of the positive and negative current half-wave of the *N* phase (where 1 corresponds to the phase A, 2 corresponds to the phase and 3 corresponds to the phase C), divided by the value of the period of current signal. The period is equal to the velocity of the motor shaft multiplied to the pole pair number.

$$\left.\begin{array}{l} \left|I_{av}^{A}\right|, \left|I_{av}^{B}\right| > 1\text{Amps} \\ \left|I_{av}^{C}\right| > 2\text{Amps} \\ I_{av}^{A}, I_{av}^{B} > \langle 0 \rangle \wedge I_{av}^{C} < \langle 0 \rangle \end{array}\right\} \text{Transistor is shorted} \quad (4)$$

$$\left.\begin{array}{l} \left|S_{+}^{1} + S_{-}^{1}\right| > 0{,}01\left(\left|S_{+}^{1}\right| + \left|S_{-}^{1}\right|\right) \\ \left|S_{+}^{1} + S_{-}^{1}\right| < 0{,}1\left(\left|S_{+}^{1}\right| + \left|S_{-}^{1}\right|\right) \\ \left|S_{+}^{2} + S_{-}^{2}\right| > 0{,}01\left(\left|S_{+}^{2}\right| + \left|S_{-}^{2}\right|\right) \\ \left|S_{+}^{2} + S_{-}^{2}\right| < 0{,}1\left(\left|S_{+}^{2}\right| + \left|S_{-}^{2}\right|\right) \\ \left|S_{+}^{3}\right| = \langle 0 \rangle \wedge \left|S_{-}^{3}\right| > 50 \cdot \left|S_{+}^{3}\right| \end{array}\right\} \text{Transistor is open} \quad (5)$$

The numerical relations are derived empirically for these parameters of the inverter and the PMSM and checked at various assigned gammas for PWM. For the remaining phases of the motor the ratios are derived in a similar way.

On the basis of these algorithms the m-functions to analyze the phase current waveforms were developed in Matlab software. Using these functions, a set of arrays with currents at various operating modes was analyzed. Each function manifested the corresponding fault and did not trigger at other fault types or in the healthy mode. Thus, the check has showed that the algorithms have a sufficient selectiveness, i.e. do not triggered at other faults in operation, and a sufficient sensitivity, triggering when a detectable fault appears at various reference to the PWM module.

5 Conclusion

Approaches for determining faults of a voltage inverter supplying power to a permanent magnet motor using FFT and without it have been discussed. Suggested in 4.3 algorithms allow a type of fault in the electric drive inverter to be securely identified when the rotor is stopped or when the rotor is moving with constant speed.

They are applicable as test ones to check the technical state of the drive power subsystem before the positioning of a telescope and the working out of an operating program. It is also possible to use them

ISBN: 978-960-474-371-1

for diagnosing an electric drive after a contingency occurs to reduce the time for localization of an emergency, repair, and putting the electric drive into operation.

Acknowledgement

This work was financially supported by Government of Russian Federation, Grant 074-U01.

References:

[1] V.A.Sinitsyn, V.S.Tomasov, Power Subsystems of Follow-Up Electric Drives of Measuring Telescopes. *News of Higher Education Establishments. Priborostroyeniye*. Vol.51, No.6, 2008, pp. 12-17.

[2] D.K.Kastha, B.K.Bose, Investigation of Fault Modes of Voltage-Fed Inverter System for Induction Motor Drive, *Industry Applications Society Annual Meeting*, IEEE, 1992., vol.1, , pp.858-866.

[3] J.A.A.Caseiro, A.M.S.Mendes, A.J.M.Cardoso, Fault Diagnosis on a PWM Rectifier AC Drive System with Fault Tolerance Using the Average Current Park's Vector Approach, *Electric Machines and Drives Conference*, IEEE International, 2009 , pp. 695-701.

[4] R.Supangat, N.Ertugrul, W.L.Soong, D.A.Gray, C.Hansen, J.Grieger, Broken Rotor Bar Fault Detection in Induction Motors Using Starting Current Analysis, *Power Electronics and Applications*, European Conference on, 2005, pp.10

[5] Czeslaw T. Kowalski, Teresa Orlowska-Kowalska, Neural Networks Application for Induction Motor Faults Diagnosis, *Mathematics and Computers in Simulation*, Vol.63, Issues 3–5, 2003, pp. 435-448.

[6] C.Concari, G. Franceschini, C.Tassoni, Rotor Fault Detection in Closed Loop Induction Motors Drives by Electric Signal Analysis, *18th International Conference on Electrical Machines*, 2008, pp.6-9.

[7] A.G. Jimenez, A.O. Munoz, M.A. Duarte-Mermoud, Fault Detection in Induction Motors Using Hilbert and Wavelet Transforms, *Electrical Engineering*, Vol.89, No.3, 2007, pp. 205-220.

[8] K.S. Gaeid, H. W. Ping, M. Khalid, A. Lauy Salih, Fault Diagnosis of Induction Motor Using MCSA and FFT, *Electrical and Electronic Engineering*, Vol.1, No.2, 2011, pp. 85-92.

[9] C. Marcelo, J. P. Fossatti, J.I. Terra, Fault Diagnosis of Induction Motors Based on FFT, *Fourier Transform - Signal Processing*, Intechopen, 2012.

[10] M.Frigo, S.G.Johnson, FFTW: An Adaptive Software Architecture for the FFT, *Proceedings of the International Conference on Acoustics, Speech, and Signal Processing*, Vol.3, 1998, pp. 1381-1384.

[11] J.Quiroga, Li Liu, D.A.Cartes, Fuzzy Logic Based Fault Detection of PMSM Stator Winding Short Under Load Fluctuation Using Negative Sequence Analysis, *American Control Conference*, 2008, pp.4262-4267.